Quantum lattice motion and optical absorption in conjugated polymers: adiabatic theory

Mostovoy, Maxim; Knoester, Jasper

Published in:
Physical Review B

DOI:
10.1103/PhysRevB.53.12057

Publication date:
1996

Quantum lattice motion and optical absorption in conjugated polymers: Adiabatic theory

Maxim V. Mostovoy* and Jasper Knoester
Institute for Theoretical Physics, Materials Science Center, University of Groningen, Nijenborgh 4, 9747 AG Groningen, The Netherlands
(Received 10 October 1995)

The quantum lattice motion of short conjugated polymer chains ($N \leqslant 70$) described by the Su-Schrieffer-Heeger (SSH) model is studied within the adiabatic approximation. We find that for these short chains only three lattice degrees of freedom are strongly affected by low-energy electronic transitions. Moreover, we show that for $N \leqslant 30$ these three degrees of freedom are only weakly coupled to each other. This allows us to perform a calculation of the optical-absorption spectrum of polymer chains in which the lattice is treated quantum mechanically rather than (semi)classically. For the standard set of SSH parameters for *trans*-polyacetylene, the classical (rigid-band) absorption edge is smeared over an energy interval of 0.5 eV by the lattice quantum fluctuations. The validity of the adiabatic approximation is investigated. Finally, we find a strong size dependence of the onset of the optical-absorption spectrum.

I. INTRODUCTION

Over the past decades, considerable effort of physicists and chemists has been devoted to understanding and optimizing the properties of conjugated polymers.[1] Much interest in these materials was aroused by the observed drastic increase of the conductivity upon doping.[2] In addition, a large number of studies have focused on the (nonlinear) optical response of conjugated polymers. In particular the strong scaling of their optical hyperpolarizabilities with the electron conjugation length continues to attract much interest.[3] Polymer light emitting diodes (LED's) are among the promising applications, for which both optical and transport properties are important.[4]

The electronic properties of conjugated polymers differ considerably from those of conventional inorganic semiconductors, mainly as a result of the specific effects arising from the interaction of itinerant electrons with a quasi-one-dimensional lattice. In 1979, Su, Schrieffer, and Heeger[5,6] proposed a model (the SSH model) that explained the existence of spinless charge carriers in polyacetylene, as was suggested by earlier experiments.[7] In this model, the electron-phonon interaction (i) relates the band gap in the undoped polymer to the lattice dimerization, (ii) leads to a strong dressing of the electronic excitations (polarons), and (iii) results in the appearance of excitations of an entirely different nature (solitons). According to this picture, a change in the occupation of the one-electron levels in a conjugated polymer, induced by photon absorption or doping, is accompanied by strong lattice deformations, that considerably change the energies of the one-electron levels. Consequently, even if direct electron-electron interactions are neglected, it is impossible to characterize the excited states of conjugated polymers by the simple concepts of fixed one-electron bands and band gaps.

In this paper, we will study the optical-absorption spectrum of conjugated polymers, accounting for the quantum nature of the lattice. Within a classical treatment, the lattice is initially fixed in the configuration that minimizes the total ground-state energy. Moreover, a classical lattice cannot readjust instantaneously to an electronic transition, so that the band gap caused by the ground-state lattice dimerization defines a sharp lower edge in the optical-absorption spectrum. Experimentally, such a sharp edge is not observed. As was pointed out by Sethna and Kivelson,[8] however, absorption can take place at photon frequencies well below this classical edge (''subgap'' absorption), provided that the electronic transition is accompanied by the creation of a soliton-antisoliton pair in the lattice. This process is classically forbidden, but quantum fluctuations of the lattice make it possible. Like in molecular spectroscopy, the absorption probability is determined by the overlap between the initial and final lattice wave functions (the Franck-Condon factor), which results in a smearing of the absorption edge.

Lattice quantum fluctuations are important as a result of the small value of the average dimerization: about 0.04 Å for trans-polyacetylene. Quantum Monte Carlo simulations have shown that the fluctuations of the dimerization are of the same order.[9,10] Since within the SSH model the gap is related to the dimerization, it is obvious that the quantum lattice motion strongly affects the optical-absorption spectrum. Unfortunately, quantum Monte Carlo calculations cannot give direct information about the excited states (or the dynamical correlation functions) necessary to obtain the absorption spectrum.

Clearly, owing to the large number of lattice degrees of freedom for realistic size polymers, a full quantum description of the coupled lattice-electron dynamics is prohibitively complicated, forcing one to apply approximations. Close to the threshold for soliton-antisoliton pair creation, the final wave function describing lattice fluctuations around the classical configuration with minimal energy (corresponding to an infinitely separated soliton-antisoliton pair) only has very small overlap with the initial wave function, describing zero-point fluctuations around the perfectly dimerized lattice. This suppresses the transition probability and enables one to calculate the absorption close to the threshold semiclassically.[8,11,12] In this approach, the overlap integral can be written $C \exp(-S_i/\hbar)$, where S_i is the action of the classical motion in the imaginary time along the trajectory connecting initial and final lattice configurations (the instanton). The preexponential factor C can be related to the sta-

bility properties of this trajectory and accounts for the contributions of the paths close to the classical one.

Using a path-integral approach, Kivelson and Auerbach[13] developed a general formalism that allows for the semiclassical calculation of the Franck-Condon factors between lattice states in the electronic ground and excited states. When applying this formalism to calculate the ''subgap'' absorption,[11] however, these authors assumed for the (analytically unknown) instanton trajectory an approximation, that simply interpolates between the perfectly dimerized configuration and the soliton-antisoliton pair and has only one degree of freedom: the soliton-antisoliton distance. This trajectory does allow for analytical results, but it is not the real solution of the classical equations of motion and, therefore, makes a proper calculation of the preexponential factor impossible. The validity of this approach is limited to photon energies lying in a small interval close to the soliton-antisoliton pair threshold.

The subgap absorption has also been calculated within a ''lattice relaxation'' approach.[14] In that work, the lattice dynamics was assumed to be linear and the phonon frequencies were considered independent of the occupation of the single-electron levels. More precisely, the only effect of electronic excitations on the lattice was assumed to be a shift of the minimum of its effective potential energy to a new configuration. This shift results in a nonzero overlap of the initial state with final states containing a number of phonon excitations over the new vacuum (multiphonon emission). Using this concept, the absorption spectrum for the continuum version of the SSH model was calculated. It should be noted, however, that in the continuum limit the linear approximation for the lattice dynamics is not justified, as the optical absorption involves large lattice fluctuations (such as soliton-antisoliton pairs), which cannot be described in terms of harmonic oscillations.

From the above, it may be concluded that the role of quantum lattice fluctuations on the optical absorption, although understood qualitatively, has only partially been solved quantitatively. This problem has recently gained further interest, as it has been suggested by Heeger and coworkers that quantum fluctuations are responsible for the large third-order optical response in degenerate-ground-state conjugated polymers.[15–18] Therefore, in this paper we reconsider the problem of the quantum description of the lattice and its influence on the optical absorption. We focus on the lattice dynamics accompanying the optical absorption in relatively short polymer rings (several tens of monomers) and show that it is quite different and much simpler than in the case of infinite chains. This is a consequence of the fact that only a few relevant lattice degrees of freedom, described in terms of phonons with wave vectors close to π, are coupled strongly to the electron dynamics. The weak coupling between the relevant degrees of freedom allows us to perform the full quantum-mechanical calculation, similar to Ref.14, retaining, however, the essential nonlinearity of the lattice dynamics and its dependence on the occupation of the single-electron levels. Apart from this quantum calculation, we also analytically solve for the instanton path and show that a proper calculation of the preexponential factor for a small range of photon energies gives a reasonable description of the multiphonon emission accompanying the absorption.

Surprisingly, the chain lengths that can be considered in this way are long enough to make our study relevant to experimental conditions, where the conjugation length is generally limited by defects and conformational disorder. The transition from the simple lattice dynamics to the dynamics of the continuum limit is smooth and in the case of polyacetylene occurs near $N=70$. Our results show strong size dependence which is important for the interpretation of experimental data.

The organization of this paper is as follows. In Sec. II we describe the model Hamiltonian and the adiabatic approximation. In Sec. III A, we present the results of a numerical analysis of the effective potential energies for short chains, while in Sec. III B we derive their key features analytically. Section IV contains the details and the results of the quantum-mechanical calculation of the optical-absorption spectrum, while the semiclassical approximation is considered in Sec. V, postponing some details to the Appendix. Finally, our results and conclusions are summarized in Sec. VI.

II. SSH HAMILTONIAN AND ADIABATIC APPROXIMATION

We will calculate the linear absorption spectrum for polymer chains described by the SSH model,[5,6] in which the electron-lattice interaction is introduced through the dependence of the electron hopping amplitude on the carbon-carbon bond length and the Coulomb interaction between the electrons is neglected. Although this model can be used to describe various kinds of polymers, we will consider the generic example of trans-polyacetylene, $(CH)_N$, and throughout this paper use parameter values appropriate for this compound. The Hamiltonian reads

$$H_{\mathrm{SSH}}=-\sum_{n,\sigma}\left[t_0+\alpha(u_n-u_{n+1})\right](c^{\dagger}_{n+1,\sigma}c_{n,\sigma}+c^{\dagger}_{n,\sigma}c_{n+1,\sigma})+\sum_{n}\left(\frac{P_n^2}{2M}+\frac{K}{2}(u_{n+1}-u_n)^2\right), \tag{2.1}$$

where, $c^{\dagger}_{n,\sigma}$ and $c_{n,\sigma}$ are the Fermi creation and annihilation operators, respectively, for an electron with spin projection σ in the π orbital of the nth carbon atom ($n=1,\ldots,N$) and u_n is the displacement along the chain of the nth atom from its position in the undimerized chain. Furthermore, P_n denote the momenta of the CH units, M is their mass, and the standard polyacetylene parameters are $t_0=2.5$ eV for the hopping amplitude in the undimerized chain, $\alpha=4.1$ eV/Å for the electron-phonon coupling, and $K=21$ eV/Å^2 for the spring constant. The lattice dynamics of the SSH model differs fundamentally for chains with even and odd numbers of molecules. In this paper, we will restrict ourselves to even N, which is also the most likely case in realistic samples, for reasons of chemical stability (avoidance of radicals) and synthesis. Furthermore, we impose periodic boundary conditions: $u_{n+N}=u_n$ and $c_{n+N}=c_n$. This simplifies the calculation, but also leads to an artificial dependence on the divisibility of N by 4, related to the fact that the degeneracy

of the highest occupied single-electron level in the half-filled chain depends (for a fixed lattice configuration) on whether $N=4k$ or $N=4k+2$. Since we do not want to complicate the paper by considering both cases in full detail, we will throughout this paper assume that $N=4k+2$ and only briefly discuss the other case in Sec. VI. Finally, we will only consider undoped, i.e., half-filled chains.

We now turn to the general expression for the linear absorption coefficient of an ensemble of randomly oriented noninteracting chains. Assuming that initially each chain is in the ground state $|i\rangle$ (zero temperature), the absorption coefficient is given by

$$\alpha(\omega)=\frac{4\pi^2\omega}{3c\,\eta}n_{\rm ch}\sum_f |\langle f|\hat{\mathbf{d}}|i\rangle|^2\delta(E_f-E_i-\hbar\omega), \quad (2.2)$$

where the sum over final states f extends over all excited states of the chain, and $\hat{\mathbf{d}}$ is the electron dipole operator. E_i and E_f denote the energies of the initial and final states, respectively, ω is the photon frequency, $n_{\rm ch}$ is the density of polymer chains, and η is the refractive index.

In order to evaluate Eq. (2.2), we have to calculate the eigenstates $\Psi(\mathbf{n},\mathbf{u})$ for the $N\pi$ electrons and the N carbon atoms governed by the SSH Hamiltonian. Here, $\mathbf{n}=(n_1,n_2,\ldots,n_N)$ is a vector containing the positions of the electrons and $\mathbf{u}\equiv(u_1,u_2,\ldots,u_N)$ is the vector of displacements of the CH units. We will restrict ourselves to the adiabatic approximation, the validity of which will be discussed in Sec. III B. Within this approximation, the total wave function is factored as

$$\Psi(\mathbf{n},\mathbf{u})=\chi(\mathbf{n}|\mathbf{u})\Phi(\mathbf{u}), \quad (2.3)$$

where $\chi(\mathbf{n}|\mathbf{u})$ is a Slater determinant of N single-electron wave functions at a given lattice configuration $\mathbf{u}$, and $\Phi(\mathbf{u})$ is the lattice wave function. The $2N$ possible single-electron wave functions $\psi_a(n|\mathbf{u})$ and their energies $\varepsilon_a(\mathbf{u})$ are found by diagonalizing the hopping term of the Hamiltonian at fixed value of $\mathbf{u}$ (the label a also includes the spin projection). This amounts to a simple numerical $N\times N$ matrix diagonalization. Of course, $(2N!)/(N!)^2$ different Slater determinants can be made, differing in the occupation of the single-electron levels. In order not to complicate the notation, however, we have not explicitly labeled $\chi(\mathbf{n}|\mathbf{u})$ by this occupation.

The lattice wave function $\Phi(\mathbf{u})$ satisfies the Schrödinger equation

$$\left(-\frac{\hbar^2}{2M}\sum_n\frac{\partial^2}{\partial u_n^2}+U(\mathbf{u})\right)\Phi(\mathbf{u})=E\Phi(\mathbf{u}), \quad (2.4)$$

where the effective potential energy $U(\mathbf{u})$ is the sum of the energies of the occupied electron levels and the harmonic energy of the lattice

$$U(\mathbf{u})=\sum_{\rm occ\ a}\varepsilon_a(\mathbf{u})+\frac{K}{2}\sum_n (u_{n+1}-u_n)^2. \quad (2.5)$$

We note that in a more rigorous treatment Eq. (2.4) should be replaced by[19,20]

$$\left[\frac{1}{2M}\left(\frac{\hbar}{i}\frac{\partial}{\partial\mathbf{u}}-\mathbf{A}(\mathbf{u})\right)^2+U(\mathbf{u})+\phi(\mathbf{u})\right]\Phi(\mathbf{u})=E\Phi(\mathbf{u}). \quad (2.6)$$

However, the effective vector potential $\mathbf{A}(\mathbf{u})=i\hbar\Sigma_{\mathbf{n}}\chi^{\dagger}(\mathbf{n}|\mathbf{u})(\partial/\partial\mathbf{u})\chi(\mathbf{n}|\mathbf{u})$ vanishes everywhere, because all electron wave functions can be chosen real. The effective scalar potential $\phi(\mathbf{u})$ is significant only in the regions of the lattice configuration space where the single-electron levels cross and the adiabatic approximation fails. As for low-energy lattice excitations the wave function is small in these regions, the scalar potential can be neglected.

Next, we consider the matrix elements of the electron dipole operator, $\hat{\mathbf{d}}=e\Sigma_{n,\sigma}\mathbf{x}_n c_n^{\dagger}c_n$, where $\mathbf{x}_n$ is the position of the nth carbon atom and e is the electron charge. As $\hat{\mathbf{d}}$ is a single-electron operator, it will, within the adiabatic approximation, only induce transitions between two Slater determinants that differ by precisely one occupied single-electron level. Explicitly, consider the transition in which an electron is transferred from an initially occupied single-electron level a to an unoccupied level b, while the lattice makes a transition from state A to state B. The dipole matrix element for this transition is easily found to be

$$\langle f|\hat{\mathbf{d}}|i\rangle=\int d^N u\,\Phi_B^*(\mathbf{u})\mathbf{D}^{ba}(\mathbf{u})\Phi_A(\mathbf{u}), \quad (2.7)$$

with

$$\mathbf{D}^{ba}(\mathbf{u})=e\sum_n \psi_b^*(n|\mathbf{u})\mathbf{x}_n\psi_a(n|\mathbf{u}). \quad (2.8)$$

Clearly, the electronic matrix element $\mathbf{D}^{ba}(\mathbf{u})$ depends on the shape of the chain, which we will assume to be circular with radius $R=Na_0/2\pi$, where $a_0=1.22$ Å is the distance between the carbon atoms in polyacetylene measured along the chain. If we choose the coordinate system such that the ring lies in the xy plane, $\mathbf{D}^{ba}(\mathbf{u})$ only has two nonzero components,

$$D_1^{ba}(\mathbf{u})=e\sum_{n=1}^{N}\psi_b^*(n|\mathbf{u})R\cos(\theta_n)\psi_a(n|\mathbf{u}), \quad (2.9a)$$

and

$$D_2^{ba}(\mathbf{u})=e\sum_{n=1}^{N}\psi_b^*(n|\mathbf{u})R\sin(\theta_n)\psi_a(n|\mathbf{u}), \quad (2.9b)$$

with

$$\theta_n=\frac{na_0+u_n}{R}=2\pi\left(\frac{n}{N}+\frac{u_n}{a_0N}\right), \quad (2.10)$$

the angle characterizing the position of the nth atom in the ring. Deformation of the chain from a perfect circle does not lead to qualitative changes in the absorption spectrum. For a proper definition of the dipole operator, however, it is crucial that the chosen geometry is consistent with the boundary conditions imposed on the wave functions. For instance, choosing $\mathbf{x}_n=na_0\mathbf{e}$, with $\mathbf{e}$ a fixed vector, is not consistent with our periodic boundary conditions and gives an absorption spectrum that looks considerably different from that for a linear chain with open boundary conditions.

If the lattice is treated classically, being fixed in the configuration that minimizes the adiabatic ground-state energy, the absorption spectrum of a *long* chain shows a sharp lower edge corresponding to the gap between the conduction and valence bands. Within the same approximation, the spectrum of a *short* chain consists of a number of well separated peaks. In both cases the onset of the absorption corresponds to the transition from the highest occupied single-electron state to the lowest unoccupied one. In this paper, we are interested in the spectral broadening of this lowest-energy transition peak due to quantum lattice fluctuations. We will assume that initially the lattice is in its ground state (zero temperature). In the final state, however, we have to account for possible excitations of the lattice accompanying the electronic transition. Unless stated otherwise, we will hereafter use the term ''electronic ground state'' for the electron configuration where all single-electron levels below the Fermi level are filled and all others are empty. By ''electronic excited state,'' we will mean the state generated from the ground state by transferring one electron from the highest occupied to the lowest unoccupied level.

III. ADIABATIC POTENTIALS FOR SHORT CHAINS

A. Numerical analysis

Whereas the calculation of the single-electron states is a straightforward numerical problem, finding the lattice wave functions $\Phi(\mathbf{u})$ for a given electron occupation is immensely complicated, as it involves solving the Schrödinger equation in an N-dimensional configuration space. We shall show, however, that for relatively short polymer chains ($N<70$) the number of lattice degrees of freedom excited by low-energy photons is small. This considerably simplifies the calculation of the optical absorption. It should be stressed that restricting ourselves to short chains does not necessarily limit the relevance to practical circumstances. The reason is that, although polymer chains can be made very long, the free propagation of electrons along the chain is, due to various defects (in particular conformational disorder), limited to relatively short chain intervals, with a typical length of several tens of atoms.[21] Therefore, the description of a polymer sample as an ensemble of disconnected fully conjugated short chains may be viewed as a rough way to account for the effects of disorder. For many materials this picture seems more adequate than the infinite chain description.

Most of the analytical studies of the quantum dynamics of polymer chains have been performed in the continuum limit. The continuum version of the SSH model[22] gives a good approximation to the discrete model if two conditions hold: (i) the gap, $2\Delta_0$, is much smaller than the π-band width, given by $4t_0$, (ii) the typical distance between the neighboring single-electron levels near the Fermi energy is much smaller than the gap. While the first condition is fulfilled for trans-polyacetylene ($2\Delta_0 \approx 1.4$ eV and $4t_0 = 10$ eV), the second one requires the chain size N to be rather large: The relevant level distance for a half-filled undimerized polyacetylene chain equals $2\pi t_0/N$, which, for a gap of 1.4 eV, gives $N \gg 10$ to fulfill the second condition. Thus, an interval of chain sizes exists, which are of practical interest, but for which the continuum model is not applicable, even though $N \gg 1$. We will call such chains short.

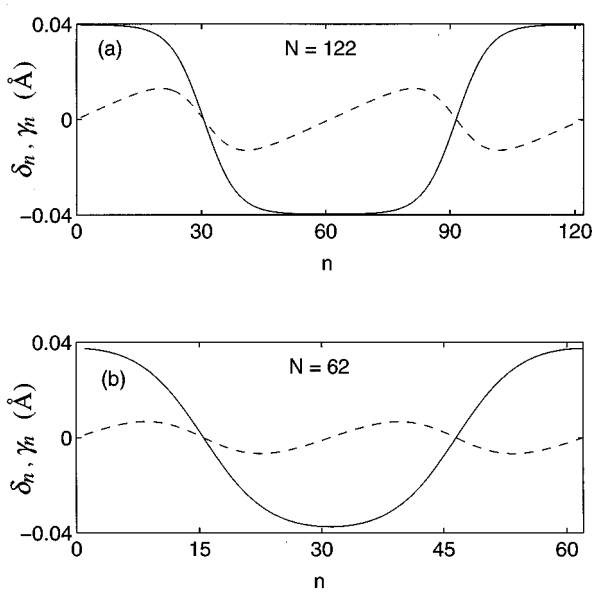

FIG. 1. Lattice configurations minimizing the effective potential energy of the lowest electronically excited state for $N=122$ (a), and $N=62$ (b). Plotted are the acoustic (γ_n, dashed line) and optical (δ_n, solid line) parts of the configuration, as defined in the text.

The lattice dynamics of short chains is quite different from those in the continuum limit. In fact, it is much simpler, because the number of the relevant lattice degrees of freedom is greatly reduced. To demonstrate this, we will compare the lattice configurations that minimize the effective potential energy of short and long electronically excited chains. For this comparison, it is necessary to introduce the phonon decomposition of the configuration,

$$u_n = \frac{1}{\sqrt{N}} \sum_k e^{ikn} q_k, \tag{3.1}$$

where $k = -\pi + 2\pi/N, -\pi + 4\pi/N, \ldots, \pi$. The phonon amplitudes $q_k = q_k' + iq_k''$ are complex, except for $k=0$ or $k=\pi$. Here we consider the amplitudes with $k \geqslant 0$ as independent variables and use $q_{-k} = q_k^*$. Furthermore, we separate u_n in slowly varying and staggering (dimerization) parts:

$$u_n = \gamma_n + (-)^n \delta_n, \tag{3.2}$$

where γ_n accounts for the acoustic phonons [Eq. (3.1) with $k<\pi/2$] and $(-)^n\delta_n$ for the optical ones ($k>\pi/2$).

The numerically obtained lattice configurations that minimize the effective potential energy of electronically excited chains with $N=122$ and $N=62$ are shown in Fig. 1, by plotting γ_n and δ_n. Clearly, both variables vary smoothly over the chains, indicating that the phonon spectrum consists of two well-separated peaks, one at small k and one at k close to π. The effective energy related to γ_n (resulting from interactions with acoustic phonons) is small, making it irrelevant for our consideration. The important part of the lattice configuration is the dimerization δ_n. From Fig. 1, it is evident that for short chains the effective potential energy has a much simpler form than for long chains: For $N=122$, the dimerization δ_n reveals a soliton-antisoliton pair, for which the phonon decomposition contains many harmonics. By contrast, the staggering part of the corresponding configura-

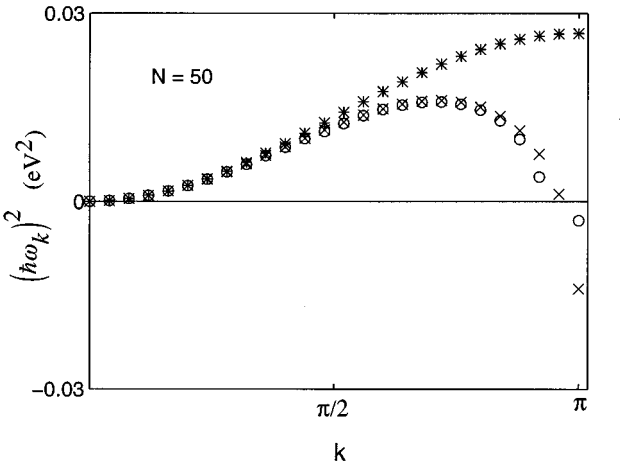

FIG. 2. Numerically obtained phonon dispersion for polyacetylene chains of 50 units in the electronic ground state (crosses), excited state (circles), and for the harmonic chain in the absence of electron-phonon interaction (asterisks). The frequency for $k=\pi(1-2/N)$ in the excited state is not defined, because the effective potential has a cusp at $q_{\pi(1-2/N)}=0$.

tion for $N=62$, basically, contains only one phonon mode with wave vector $k=\pi(1-2/N)$. This configuration may be interpreted as a dimerization wave with a period equal to the chain length. When increasing the chain length, the dimerization wave smoothly changes into a soliton-antisoliton pair at $N\approx 70$–80 (for our choice of model parameters).

Because of the charge conjugation symmetry[23] of the SSH Hamiltonian the configuration that minimizes the lowest electronically excited state of the half-filled chain also minimizes the energy of the ground state when two electrons are added or removed, in which case the dimerization wave is called a charge-density wave (CDW). Therefore, the above change of the soliton-antisoliton pair into a dimerization wave is related to the earlier found transition from a soliton lattice to a CDW when increasing the doping.[24]

Additional evidence for the reduction of the number of relevant lattice degrees of freedom is found by considering the renormalization (due to the electron-phonon interaction) of the frequencies of small amplitude oscillations around the minimum of the potential energy. In Fig. 2 we plot

$$(\hbar\omega_k)^2=\frac{\hbar^2}{M}\frac{\partial^2 U}{\partial q_k^2}\bigg|_{\mathbf{q}=0} \tag{3.3}$$

as a function of k for both the electronic ground and excited state and compare to the normal-mode dispersion in the absence of the electron-phonon interaction. Clearly, the acoustic phonons are only weakly affected by this interaction. By contrast, the frequencies of the optical phonons are reduced, but the crucial point is that most of them are nearly the same in the electronic ground and excited state. Therefore, these degrees of freedom remain practically unexcited upon electronic transitions. We have checked that the dependence of the effective potential energy on those (irrelevant) lattice coordinates is to a good approximation harmonic,

$$U_{\text{irrel}}(\mathbf{q})=\sum_{\text{irrel }k}\frac{M\omega_k^2}{2}(q_k'^2+q_k''^2), \tag{3.4}$$

where the frequencies ω_k only weakly depend on the electronic state.

A similar harmonic approximation fails for the phonon modes with wave vectors $k=\pi$ and $k=\pi(1-2/N)$. In the former case, $\omega_\pi^2<0$ in the electronic ground state, related to the familiar double-well potential which arises from the electron-phonon interaction. For $k=\pi(1-2/N)$, the potential energy in the electronic excited state has a cusp at $q_k=0$. In the remainder of this section, we will discuss the numerically obtained dependence of the effective potential energy on the three coordinates describing these relevant phonon modes. It is useful to introduce a special notation for these coordinates:

$$\begin{aligned} z&=q_\pi,\\ x+iy&=\rho e^{i\varphi}=\sqrt{2}q_{\pi(1-2/N)}. \end{aligned} \tag{3.5}$$

In addition, we define the rescaled amplitudes $\tilde{z}=z/\sqrt{N}$, and analogous for x, y, and ρ. The lattice configuration described by the vector $\mathbf{r}=(x,y,z)$ then reads

$$\delta_n=\tilde{z}+\sqrt{2}\tilde{\rho}\,\cos\left(\frac{2\pi n}{N}-\varphi\right). \tag{3.6}$$

Thus, $\tilde{z}$ is the average dimerization of the chain, $\sqrt{2}\tilde{\rho}$ is the amplitude of the dimerization wave with period equal to the chain length [cf. Fig. 1(b)], and the angle φ describes the shift of this wave along the chain. In the limit $N\to\infty$ the effective potential energy is φ independent. In the case of a finite chain, it is invariant only under the finite rotation $\varphi\to\varphi+2\pi/N$ (accompanied by $z\to -z$), which corresponds to a shift of the dimerization wave by one lattice unit. Nevertheless, for all practical purposes, the effective potential energy for a chain of several tens of units can be taken independent of φ.

From the above, we conclude that for short chains the dynamics of only two lattice degrees of freedom (z and ρ) is nontrivial. Due to the interaction with the electrons, these two phonon amplitudes will generally be coupled, which is indeed seen from the form of the effective potential energy for the electronically excited chain of 70 units, given in Fig. 3(a). In order to evaluate the optical absorption one has to calculate the wave functions of many excited lattice states in this potential, which is complicated by the coupling between the two degrees of freedom (though, of course, this problem is already much easier than solving the quantum motion in the full N-dimensional lattice configuration space).

However, it turns out that the coupling diminishes for shorter chains. This can be seen from Fig. 3(b), which displays the same potential energy for $N=30$. To a good approximation, the variables z and ρ are decoupled in the electronic excited state for this chain length. The same holds for the electronic ground state. We will make these statements more explicit by showing how along various cuts in the xz plane the numerically obtained effective potentials (for $N=30$) can be fitted by simple decoupled expressions.

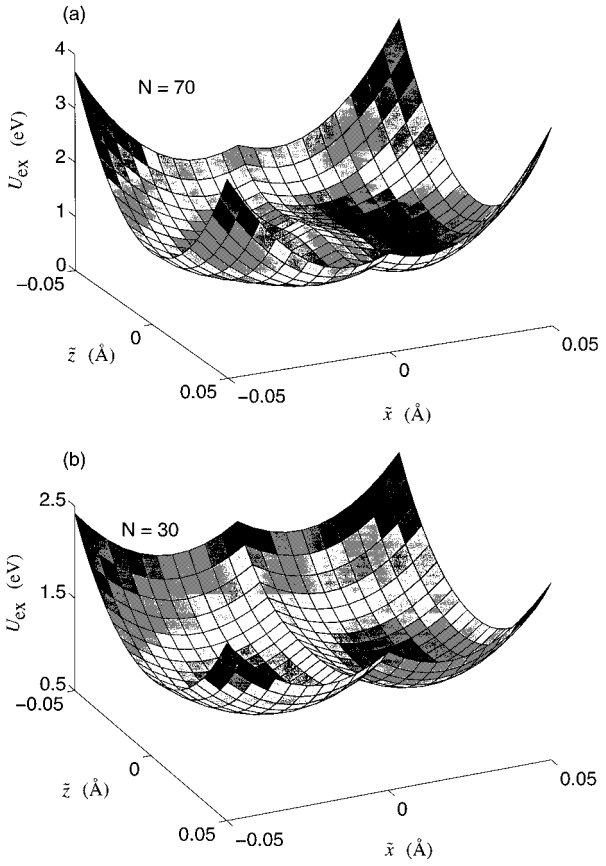

FIG. 3. Effective potential energy in the electronically excited state as a function of the two relevant phonon coordinates $\tilde{z}$ and $\tilde{x}$ for $N=70$ (a) and $N=30$ (b).

First, we consider the electronic ground state and fit its effective lattice potential by the decoupled function

$$U_{\mathrm{vac}}(\rho,z)=\frac{M\omega_{\perp}^{2}\rho^{2}}{2}+V_{\mathrm{vac}}(z), \tag{3.7}$$

where $V_{\mathrm{vac}}(z)$ is a double well with minima at $\pm a$, with a related to the classical value of the dimerization u_0 through $a=\sqrt{N}u_0$. Figure 4 shows the numerically obtained potential, as well as the fit along three cuts in the xz plane. We determined $V_{\mathrm{vac}}(z)$ by fitting $U_{\mathrm{vac}}(0,z)$ by an eighth-order polynomial [Fig. 4(a)]. Likewise, the frequency $\omega_{\perp}$ was found from a quadratic fit of $U_{\mathrm{eff}}(\rho,0)$ [Fig. 4(b)]. Finally, in Fig. 4(c), the thus obtained form Eq. (3.7) is compared to the exact effective potential along the cut $z+\rho=a$. Clearly, the fit is satisfactory in the region where the ground-state lattice wave function (also indicated in the figure) is appreciable.

Similarly we fitted the effective potential energy for the electronic excited state [cf. Fig. 3(b)] by the expression

$$U_{\mathrm{ex}}(\rho,z)=\Delta U+V_{\mathrm{ex}}(\rho)+\frac{M\omega_{\parallel}'^{2}z^{2}}{2}, \tag{3.8}$$

with

$$V_{\mathrm{ex}}(\rho)=\frac{M\omega_{\perp}'^{2}}{2}(\rho-b)^{2},\quad \rho\geqslant 0. \tag{3.9}$$

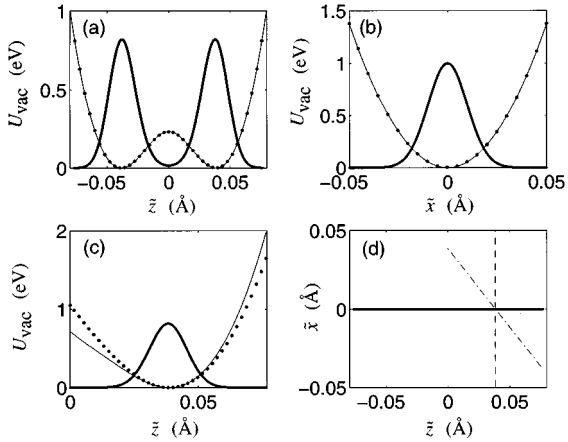

FIG. 4. Effective potential energy U_{vac} of the electronic ground state for $N=30$ according to exact numerical calculation (thin solid line) and the fit Eq. (3.7) (dots) along three cuts in the xz plane. The cut directions are indicated in panel (d) and are given by $\tilde{x}=0$ (a), $\tilde{z}=a/\sqrt{N}$ (b), and $\tilde{x}+\tilde{z}=a/\sqrt{N}$ (c), where $a/\sqrt{N}$ is the ground-state dimerization. The thick solid lines give (in arbitrary units) the ground-state wave function of the lattice in the potential U_{vac} along the same cuts.

The fit is compared to the exact numerical result in Fig. 5 and again demonstrates the effective decoupling of the phonon degrees of freedom.

The minimum of the effective potential for the electronically excited state is reached at $z=0$ (zero average dimerization) on a circle

$$\rho^{2}=x^{2}+y^{2}=b^{2}. \tag{3.10}$$

The degeneracy of this minimum corresponds to the possibility of shifting the dimerization wave along the polymer. The cusp at $\rho=0$ is an artifact of the periodic boundary conditions. Although the actual z dependence of U_{ex} is slightly anharmonic, we prefer to use a quadratic fit to sim-

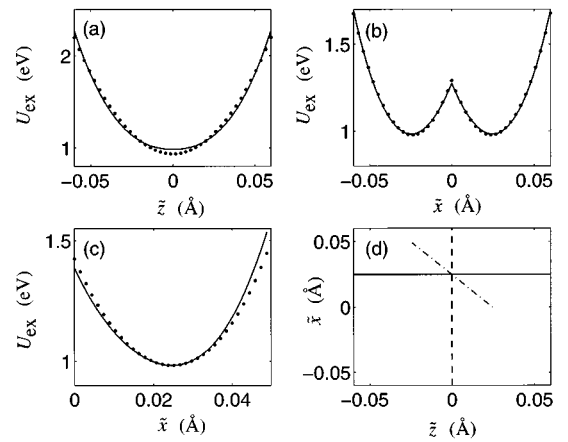

FIG. 5. Effective potential energy U_{ex} of the electronic excited state for $N=30$ according to exact numerical calculation (thin solid line) and the fit Eq. (3.8) (dots) along three cuts in the xz plane. The cut directions are indicated in panel (d) and are given by $\tilde{x}=b/\sqrt{N}$ (a), $\tilde{z}=0$ (b), and $\tilde{x}+\tilde{z}=b/\sqrt{N}$ (c), where b is the position of the minimum of the potential in the transverse ($\tilde{x}$) direction.

plify the calculation of the wave functions [see Eq. (3.16) for a more accurate expression]. The difference ΔU between the minima of the effective potential energies for the electronic excited and ground states is the threshold for optical absorption (if we discard corrections due to the small changes in the zero point phonon energies), which for the infinite chain is equal to twice the soliton mass.

B. Analytical discussion

In this section, we will present analytical arguments that explain the origin of and put a firmer basis under the simple behavior of the effective potential energies for short polymer chains found in Sec. III A. In the adiabatic approximation the coupling between the electron and phonon degrees of freedom is caused by the dependence of the adiabatic potential on the sum of the energies of the occupied single-electron levels [Eq. (2.5)]. For short chains, the separation between the single-electron levels is large and we may use perturbative arguments to build intuition about the effects of lattice distortions. Then, the largest shifts in the electron levels arise from the mixing of adjacent levels by the electron-phonon interaction. If both neighboring levels are filled, however, this will not change the effective potential. Thus, the effective potential is most sensitive to lattice distortions that couple the occupied and unoccupied single-electron levels that are close to the Fermi energy (0 for half-filling). In the undimerized chain these are the electron states with wave vectors close to $\pm\pi/2$.

From these arguments and the form of the electron-phonon interaction

$$H_{\text{e-ph}}=\frac{2i\alpha}{\sqrt{N}}\sum_{k,k',\sigma}(\sin k'-\sin k)c^{\dagger}_{k',\sigma}c_{k,\sigma}q_{k'-k}, \qquad (3.11)$$

it follows that the lattice degrees of freedom most strongly coupled to the electron dynamics are phonons with wave vectors close to π. This also holds in the continuum limit, but for a short chain the number of single-electron levels that lie in an energy interval of the order Δ_0 near the Fermi energy is very small, and so is the number of relevant phonon degrees of freedom.

We can even obtain analytical expressions which give a good semiquantitative description of the effective potential energies, by assuming that the nonlinearity of the potentials is solely related to the energies of the four (without accounting for spin degeneracy) single-electron levels closest to the Fermi energy, which we denote by $\bar{2}$, $\bar{1}$, 1, and 2. The levels 1 and 2 have positive energy and are empty in the electronic ground state, while the negative energy levels $\bar{1}$ and $\bar{2}$ are doubly occupied. Due to charge conjugation symmetry of the SSH Hamiltonian $\varepsilon_{\bar{1}}=-\varepsilon_1$ and $\varepsilon_{\bar{2}}=-\varepsilon_2$.

For an undimerized chain with N indivisible by 4, the states 1 and 2 are plane waves with wave vectors $\pm\pi(1/2+1/N)$ and equal energies $\varepsilon_{1,2}=2t_0\sin(\pi/N)$, and the degenerate states $\bar{1}$ and $\bar{2}$ are plane waves with wave vectors $\pm\pi(1/2-1/N)$. If we leave all other electron levels out of consideration, the energies of the four levels in an arbitrarily distorted chain only depend on the amplitudes of the phonons with wave vectors $\pi, \pi(1-2/N)$, and $2\pi/N$. The coupling to the acoustic phonon with wave vector $2\pi/N$ is small [cf. Eq. (3.11)] and can be neglected, while the remaining phonon degrees of freedom are our x, y, and z coordinates. Diagonalizing the Hamiltonian within the subspace of the four electron states, we obtain the energies of the single-electron levels in the presence of the lattice deformation:

$$\varepsilon_1(\rho,z)=-\varepsilon_{\bar{1}}(\rho,z)=\sqrt{A^2+2(Bz)^2}-B\rho,$$
$$\varepsilon_2(\rho,z)=-\varepsilon_{\bar{2}}(\rho,z)=\sqrt{A^2+2(Bz)^2}+B\rho, \qquad (3.12)$$

with

$$A=2t_0\sin\frac{\pi}{N},\quad B=2\sqrt{\frac{2}{N}}\alpha\cos\frac{\pi}{N}. \qquad (3.13)$$

As we see, the energy of each of the four single-electron levels is the sum of two terms, one of which depends only on z and the other only on ρ. Thus, any coupling between these two phonon degrees of freedom is completely due to the z and ρ dependence of the energies of other, deep lying, electron levels and therefore has to be small. This is the underlying reason for the decoupling of the relevant degrees of freedom found in Sec. III A.

Since we have assumed that the contribution of all the other electron levels together with the harmonic energy of the lattice can be approximated by

$$U_{\text{rest}}(\rho,z)=U_0+\frac{\beta\rho^2}{2}+\frac{\gamma z^2}{2} \qquad (3.14)$$

(with U_0, β, and γ constants), the effective potential energy of the electronic ground state reads

$$U_{\text{vac}}=U_{\text{rest}}+2(\varepsilon_{\bar{1}}+\varepsilon_{\bar{2}})$$
$$=U_0+\frac{\beta\rho^2}{2}+\frac{\gamma z^2}{2}-4\sqrt{A^2+2(Bz)^2}, \qquad (3.15)$$

and the energy of the state with one electron in level 1 and one hole in level $\bar{1}$ is,

$$U_{\text{ex}}=U_{\text{vac}}+2\varepsilon_1$$
$$=U_0+\frac{\beta\rho^2}{2}-2B\rho+\frac{\gamma z^2}{2}-2\sqrt{A^2+2(Bz)^2}. \qquad (3.16)$$

Note that the coefficient in front of $-\sqrt{A^2+2(Bz)^2}$ is smaller by a factor of two in U_{ex} compared to U_{vac}, which results in the disappearance of the nontrivial minimum at $z\neq 0$ in the excited state [cf. Figs. 4(a) and 5(a)]. On the other hand, due to the linear term $-2B\rho$, U_{ex} obtains a nontrivial minimum at $\rho\neq 0$ [cf. Fig. 5(b)].

The term $-2B\rho$ also leads to nonanalytic behavior of U_{ex}: in the x-y plane it has a cusp at $x=y=0$. This singularity is due to the degeneracy of the single-electron states 1 and 2 at $\rho=0$, which means that the energies of the four (without accounting for spin) low-lying electron excitations with one electron in either the state 1 or 2 and one hole in either the state $\bar{1}$ or $\bar{2}$ cross at $\rho=0$. Three such excitations are dipole allowed, which means that they have spin 0 and negative charge conjugation parity. The numerically ob-

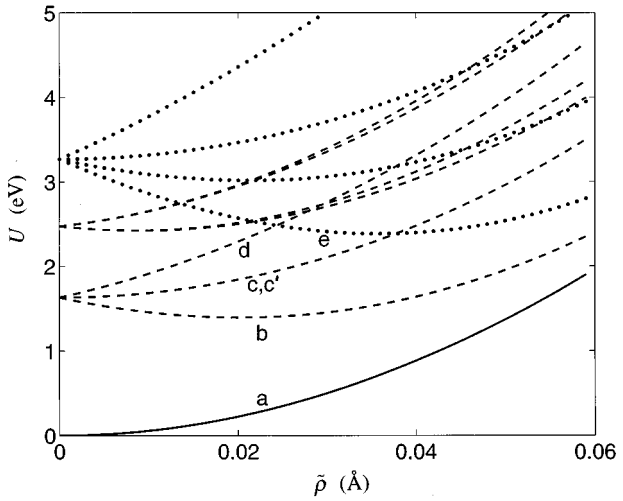

FIG. 6. The energy of the lowest electron configurations for chains of $N=30$ units as a function of $\tilde{\rho}$ (for $z=a$). The solid line indicates the electron ground state, the dashed lines denote the one-particle–one-hole states, and the dotted lines are the two-particle–two-hole states.

tained exact ρ dependence of the effective potential energies of these three excitations is shown in Fig. 6 (curves b, c, and d). According to our analytical approximation, this ρ dependence is given by

$$\Delta U+\frac{\beta\rho^2}{2}+2mB\rho, \quad m=-1,0,1. \tag{3.17}$$

In the rigid-band calculation ($z=a,\rho=0$, fixed), these three dipole transitions all would have the same energy ΔU. In the quantum calculation, the splitting of the terms at $\rho\neq 0$ contributes to the broadening of the absorption spectrum. This broadening exists in addition to the smearing of the lowest-energy electron excitation due to the possibility to also excite the lattice, which is our main focus in this paper.

At this point, we would like to discuss the validity of the adiabatic approximation for short chains. Generally, this is a good approximation if the energy of the lattice motion is small compared to the energy separation between different electron terms, so that the slow lattice motion cannot induce transitions between different electron configurations. Let us first consider the ground state of the chain (curve a in Fig. 6). The electron terms which can be nonadiabatically mixed with the ground-state electron configuration should have spin 0 and the same (positive) charge conjugation parity. The nearest two possibilities are (i) a combination of an electron in state 1 and a hole in state 2 with an electron in state 2 and a hole in state 1 (curve c' in Fig. 6, which coincides with curve c) and (ii) two electrons with opposite spin in state 1, two holes in state 1 (curve e). In the region where the ground-state lattice wave function is significant [cf. Fig. 4(b)], both of these configurations are separated from the ground state by an amount of energy considerably larger than the typical optical-phonon frequency (about 0.1 eV), which means that for the ground state the adiabatic approximation is valid. Of course, Fig. 6 only shows the ρ dependence, which is most threatening for the adiabaticity, as a result of the splitting at $\rho=0$. Inspection learns that the z dependence does not endanger the adiabatic approximation.

For the excited electron states, the situation is more problematic, however. The crossing at $\rho=0$ of the three lowest-energy excited electron terms with negative charge conjugation symmetry (curves b, c, and d in Fig. 6) gives rise to nonadiabatic transitions between them (we also note that the effective scalar potential in Eq. (2.6), which we neglected, diverges as $1/\rho$ at the terms-crossing point). Thus, only a few excited lattice states on top of the lowest-energy term (curve b) whose wave functions are localized near the minimum of the effective energy (far from $\rho=0$) can be treated adiabatically. This imposes an upper limit on the photon energy for which our results given in Sec. IV are valid, which we estimate to be 0.5 eV above the absorption threshold. The results of a full nonadiabatic treatment will be published in a forthcoming paper.

IV. QUANTUM CALCULATION OF THE OPTICAL ABSORPTION

In this section, we will apply the knowledge obtained about the adiabatic potentials and perform a full quantum calculation of the optical-absorption spectrum caused by the lowest-energy excited electron configuration. We will consider a chain of $N=30$ units, for which we have learned above that the phonons with different wave vectors are decoupled. Thus, the lattice wave function factorizes into a product of the wave functions for the separate wave vectors,

$$\Phi(\mathbf{q})=\phi_{\parallel}(z)\phi_{\perp}(\rho,\varphi)\prod_{\text{irrel }k}\phi_k(q_k',q_k''). \tag{4.1}$$

If we now neglect the weak dependence of the electron dipole matrix element on the irrelevant phonon degrees of freedom,

$$D_\alpha(\mathbf{q})\approx D_\alpha(\mathbf{r}), \tag{4.2}$$

the integration over these lattice variables in Eq. (2.7) reduces to the product of the overlap integrals of the initial (ϕ_k) and final (ϕ_k') lattice wave functions for each mode:

$$\prod_{\text{irrel }k}\int_k dq_k'dq_k''\phi_k'^{*}(q_k',q_k'')\phi_k(q_k',q_k''). \tag{4.3}$$

These integrals are easily calculated, as the irrelevant degrees of freedom are harmonic. We are interested in the optical absorption at zero temperature, so that no phonon excitations exist in the initial state. Although the phonon frequencies ω_k and ω_k' before and after the electronic transition are slightly different (see Fig. 2), it turns out that for $N=30$ the initial lattice ground state has a negligible overlap with excited final lattice states. Therefore, only transitions in which the irrelevant degrees of freedom remain unexcited are important and for these transitions the factor (4.3) equals unity.

More precisely, the phonons with small wave vectors (acoustic phonons) are weakly coupled to the electron dynamics, and the lattice configuration minimizing the energy of the polymer ring in the excited electron state has a small low-frequency component (see Fig. 1). This leads to a nonzero overlap with states in which acoustic phonons are ex-

cited. Since, however, such excitations do not cost much energy, they only result in a small broadening of the absorption peaks associated with the optical-phonon excitations. At room temperature a small additional broadening occurs due to thermal excitation of low-energy acoustic phonons in the initial state. We will not take these effects into account, since, anyway, a consistent treatment of acoustic phonons should necessarily be three dimensional.

Thus, the only nontrivial integrations in the matrix element Eq. (2.7) are the ones over the relevant degrees of freedom,

$$\int_{-\infty}^{\infty} dz\, \phi_{\parallel}'^{*}(z)\phi_{\parallel}(z) \int_{0}^{\infty} d\rho\rho \times \int_{0}^{2\pi} d\varphi \phi_{\perp}'^{*}(\rho,\varphi)\phi_{\perp}(\rho,\varphi) D_{\alpha}(\mathbf{r}). \tag{4.4}$$

We first focus on the z mode (the π phonon). The initial wave function $\phi_{\parallel}(z)$ is the symmetric ground-state wave function in the double-well potential $V_{\mathrm{vac}}(z)$ of Eq. (3.7). However, if the temperature exceeds the energy splitting due to tunneling between the degenerate minima of the potential (about 0.2 K for $N=30$), the states described by symmetric and antisymmetric lattice wave functions are populated with equal probability. For the chain sizes considered here, we may neglect the tunneling and assume that the discrete symmetry $z\rightarrow -z$ is spontaneously broken. Therefore, we have restricted ourselves to numerically calculating the lattice wave function $\phi_{\parallel}(z)$ for $z>0$. The overlap integrals with $\phi_{\parallel}'(z)$ turn out not to be sensitive to the choice of the boundary condition at $z=0$ ($\phi_{\parallel}=0$ or $d\phi_{\parallel}/dz=0$), since, in any case, the wave function is very small in the vicinity of $z=0$. Finally, according to Eq. (3.8), the wave functions $\phi_{\parallel}'(z)$ are the eigenfunctions of the harmonic oscillator with frequency $\omega_{\parallel}'$.

For the two ''perpendicular'' coordinates x and y, the situation is in a sense reversed to the above. Now, the motion is harmonic in the initial state [Eq. (3.7)] and the corresponding lattice wave function is a product of the ground-state functions for each of the two coordinates,

$$\phi_{\perp}(\rho,\varphi)=\left[\frac{2M\omega_{\perp}}{\hbar}\right]^{(1/2)} e^{-M\omega_{\perp}\rho^2/2\hbar}\frac{1}{\sqrt{2\pi}}. \tag{4.5}$$

The z component of the angular momentum of this state vanishes. Furthermore, because $V_{\mathrm{ex}}(\rho)$ does not depend on φ, the final state wave function has the form,

$$\phi_{\perp}'(\rho,\varphi)=R_{l|m|}(\rho)\frac{e^{im\varphi}}{\sqrt{2\pi}}. \tag{4.6}$$

Now note that for a circular polymer ring the matrix element of the dipole between the electron wave functions of the highest occupied and the lowest unoccupied levels transforms as a vector under rotation around the z axis,

$$D_1(z,\rho,\varphi)=D_1(z,\rho,0)\cos(\varphi)-D_2(z,\rho,0)\sin(\varphi). \tag{4.7}$$

$$D_2(z,\rho,\varphi)=D_1(z,\rho,0)\sin(\varphi)+D_2(z,\rho,0)\cos(\varphi),$$

because rotation over an angle $4\pi/N$ corresponds to a shift of the lattice configuration by two lattice units $u_n\rightarrow u_{n+2}$.

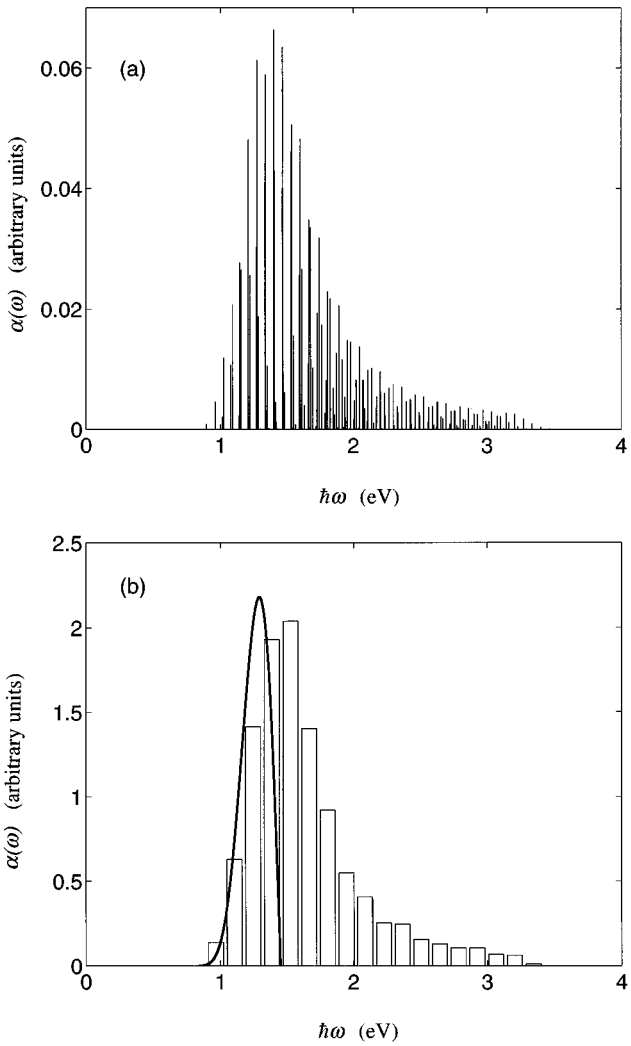

FIG. 7. (a) Stick absorption spectrum for the transition from the highest occupied to the lowest unoccupied single-electron level accompanied by various lattice excitations for a chain of $N=30$ units. Each peak derives from a particular phonon excitation and the peak height gives the relative probability for this excitation. If the lattice would be fixed in the ground-state dimerization, the spectrum would be a single δ peak at about 1.6 eV. (b) Histogram for the absorption spectrum obtained from (a) as described in the text. The solid line gives the semiclassical absorption spectrum derived in Sec. V.

Hence, the projection of the angular momentum in the final state is given by $m=\pm 1$. The wave functions $R_{l1}(\rho)$ ($l=0,1,\ldots$) of the radial excitations were found numerically.

Using the thus obtained wave functions to evaluate the matrix elements Eq. (4.4) for various phonon excitations in the excited state, we obtain as the final result of our full quantum calculation the stick spectrum Fig. 7(a). It is observed that the lowest-energy peak of the rigid-band absorption spectrum is replaced by a sequence of many peaks corresponding to different excitations of phonons with wave vectors π and $\pi(1-2/N)$. A more coarse-grained picture of the spectrum is useful for comparison with experiments and with the semiclassical approximation (Sec. V) and is obtained by making a histogram, in which the contributions from different phonon excitations inside each energy bin are

summed [Fig. 7(b)]. In this representation, the lowest (δ-shaped) rigid-band absorption peak at 1.6 eV is replaced by a broad feature due to the lattice quantum fluctuations. The onset of the absorption lies 0.7 eV below the first rigid-band transition.

V. SEMICLASSICAL CALCULATION OF THE OPTICAL ABSORPTION

In the previous section we obtained the absorption spectrum of a short polymer ring, treating the lattice quantum mechanically. For long chains, however, the number of relevant lattice degrees of freedom is large and the semiclassical (or instanton) calculation seems the best one can do. Therefore, it is instructive to compare our quantum result with the semiclassical approximation and discuss the region of validity of the latter. Although the general formulas for the absorption coefficient in the semiclassical approximation were derived in Ref. 13, we will use an equivalent but simpler approach, which exploits the fact that many phonon degrees of freedom for a short chain are decoupled and allows us to use simple WKB expressions for the wave functions rather than the path-integral approach. As in the quantum calculation, we consider only the three lattice degrees of freedom x, y, and z.

For photon energies close to the absorption threshold, the overlap between the initial and final lattice wave functions is small, because the minima of the adiabatic potentials before and after the electronic transition are located at different values of the lattice coordinates ($z=a$, $\rho=0$ for $U_{\rm vac}$ and $z=0$, $\rho=b$ for $U_{\rm ex}$). Thus, the overlap integral comes from a region where both initial and final lattice wave functions are suppressed. This means that the lattice motion is classically forbidden there and the wave functions have a WKB form

$$\phi=\sqrt{w}\,\exp(-S/\hbar), \tag{5.1}$$

where S is the action of the motion in the imaginary time in a corresponding potential from the classical turning point. The product of the wave functions $\phi_\parallel'^{*}(z)\phi_\parallel(z)\propto\exp\{-[S_\parallel'(z)+S_\parallel(z)]/\hbar\}$ has its maximum at $z=z_0$ for which the sum of the actions is minimal:

$$\frac{d}{dz}[S_\parallel(z)+S_\parallel'(z)]|_{z=z_0}=0, \tag{5.2}$$

which means that at this point the classical momenta $p_\parallel=dS_\parallel/dz$ and $-p_\parallel'=-dS_\parallel'/dz$ match. Similarly, the product of the wave functions describing the motion in the transverse direction $\phi_\perp'^{*}(\rho)\phi_\perp(\rho)\propto\exp\{-[S_\perp'(\rho)+S_\perp(\rho)]/\hbar\}$ has its maximum at ρ_0 defined by

$$p_\perp(\rho_0)=\frac{dS_\perp}{d\rho}(\rho_0)=-\frac{dS_\perp'}{d\rho}(\rho_0)=-p_\perp'(\rho_0).$$

In the semiclassical regime the classical actions are large, so that the products of the wave functions are sharply peaked. Therefore, we can calculate the matrix element Eq. (4.4) performing the integrations over z and ρ near z_0 and ρ_0 in the saddle-point approximation. The φ integral can be evaluated exactly and corresponds to the integration over the zero mode (the overall shift of the saddle-point configuration along the chain) in the continuum limit.[11] Then, the transition amplitudes into states with $m=\pm1$ are given by

$$\langle f|\hat{\mathbf{d}}|i\rangle=2\pi\rho_0\kappa|(D_1\pm iD_2)|\,\phi_\parallel'(z_0)\phi_\parallel(z_0)\phi_\perp'(\rho_0)\phi_\perp(\rho_0), \tag{5.3}$$

with

$$\kappa=2\pi\hbar\left[\frac{d}{dz}(p_\parallel'+p_\parallel)\bigg|_{z=z_0}\frac{d}{d\rho}(p_\perp'+p_\perp)\bigg|_{\rho=\rho_0}\right]^{-(1/2)}. \tag{5.4}$$

The strongest dependence of the product of wave functions in Eq. (5.3) on the ''parallel'' and ''transverse'' excitation energies $\varepsilon_\parallel'$ and $\varepsilon_\perp'$ comes from the factor $\exp[-(S_\parallel+S_\parallel'+S_\perp+S_\perp')/\hbar]$. Here, it should be noted that the sum of four actions is not yet the action along some classical path in the two-dimensional space of lattice coordinates, since the (imaginary) times of motion in the ''parallel'' and ''transverse'' directions,

$$\tau_\parallel=\frac{d(S_\parallel+S_\parallel')}{d\varepsilon_\parallel'},\qquad \tau_\perp=\frac{d(S_\perp+S_\perp')}{d\varepsilon_\perp'}, \tag{5.5}$$

are, in general, different. This will be solved automatically when performing the sum over all final states. If the spectrum of final states is dense enough, the summation can be replaced by an integration:

$$\sum_f\delta(E_f-E_i-\hbar\omega)|\langle f|\hat{\mathbf{d}}|i\rangle|^2 \approx 2\int\frac{d\varepsilon_\parallel'}{\hbar\omega_\parallel'}\frac{d\varepsilon_\perp'}{\hbar\omega_\perp'(\varepsilon_\perp')} \times\delta(\Delta U+\varepsilon_\parallel'+\varepsilon_\perp'-\hbar\omega-\varepsilon_\parallel-\varepsilon_\perp)|\langle f|\hat{\mathbf{d}}|i\rangle|^2, \tag{5.6}$$

where the factor of 2 is due to the electron spin, $\omega_\parallel'$ is defined as in Eq. (3.8), and $\omega_\perp'(\varepsilon_\perp')\equiv2\pi/\tau_\perp(\varepsilon_\perp')$, the energy separation between the states of the ''transverse'' motion of the lattice in the electronically excited state. Only the integration over the difference $\varepsilon_\parallel'-\varepsilon_\perp'$ is nontrivial, for which we again use the saddle-point approximation. Using Eq. (5.5), it is clear that for $\varepsilon_\parallel'+\varepsilon_\perp'=$ const, the factor $\exp[-2(S_\parallel+S_\parallel'+S_\perp+S_\perp')/\hbar]$ has its maximum at $\overline{\varepsilon_\parallel'},\overline{\varepsilon_\perp'}$ such that

$$\tau=\tau_\parallel(\overline{\varepsilon_\parallel'})=\tau_\perp(\overline{\varepsilon\epsilon_\perp'}), \tag{5.7}$$

which is precisely the condition for the equality of times of motion in the ''parallel'' and the ''transverse'' directions. Then, $S_i\equiv2(S_\parallel+S_\parallel'+S_\perp+S_\perp')$ becomes the instanton action and the absorption coefficient can be written as

$$\alpha(\omega)=C\,\exp(-S_i/\hbar). \tag{5.8}$$

The calculation of the classical actions $S_\parallel$, $S_\parallel'$, $S_\perp$, and $S_\perp'$ is discussed in the Appendix. The preexponential factor C has a rather lengthy expression, which agrees with the result of the path-integral method.[13]

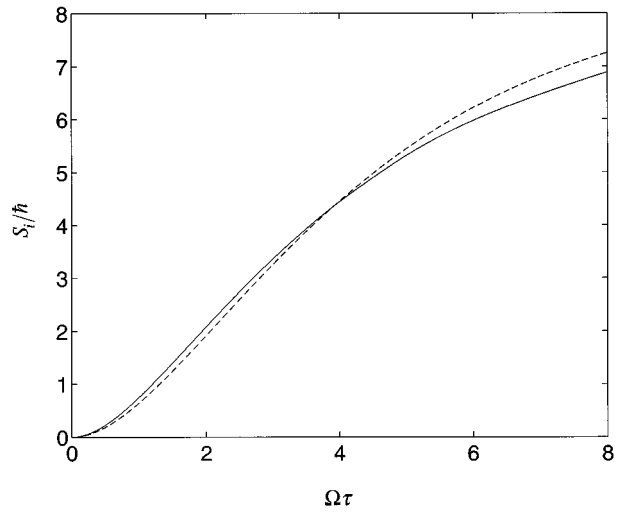

FIG. 8. Instanton action as a function of (imaginary) time of motion in the electronic excited-state potential $U_{\rm ex}$. The solid line gives the result of the numerical calculation and the dashed line was obtained analytically, using the decoupling of the phonon degrees of freedom.

In the above derivation, we neglected the coupling between the ''parallel'' and the ''transverse'' degrees of freedom. To demonstrate once more that for short chains this is a good approximation, we compared for $N=30$ the properties of our analytical instanton with those of the instanton obtained by numerically solving the classical equations of motion. In the latter calculation, we even accounted for two additional lattice degrees of freedom, the real and imaginary parts of $q_{\pi(1-4/N)}$, the amplitudes of which turned out to be relatively small. The effective lattice potentials $U_{\rm vac}$ and $U_{\rm ex}$ as functions of the five lattice variables were obtained by numerically diagonalizing the single-electron Hamiltonian. Figure 8 shows the instanton action as a function of $\Omega\tau$, where $\Omega=\sqrt{4K/M}$ is a typical optical-phonon frequency and τ is the time of motion in the adiabatic potential of the electronically excited state given by Eq. (5.7). Clearly, a good agreement exists between the analytical and the numerically obtained instanton.

The final result for the semiclassical absorption spectrum is shown in Fig. 7(b), where it is compared to the histogram of the quantum calculation. Unfortunately, just above the absorption threshold, where the suppression by the Frank-Condon factor is strong and the semiclassical approximation is supposed to be very precise, the number of available lattice excitations in a short chain is relatively small [see Fig. 7(a)], and the comparison of a smooth curve with a histogram is, strictly speaking, impossible. Still one can say that for photon energies just above the threshold, the instanton approach reasonably describes the diffusion of the onset of the absorption due to multiphonon emission accompanying the electronic transition.

At higher photon energies the instanton ideology breaks down, because the lattice fluctuations in the excited states become large and the final lattice wave function is no longer small for configurations close to the perfectly dimerized lattice. This manifests itself in a shrinking of the instanton path for increasing photon energy. The saddle-point configuration described by the coordinates (ρ_0,z_0), at which according to the semiclassical scenario the electron transition occurs, for growing photon energy tends to the perfectly dimerized configuration ($\rho_0\rightarrow 0$ and $z_0\rightarrow a$), until, finally, the instanton disappears. When this happens the saddle-point value of the transverse coordinate ρ_0 becomes zero and the semiclassical expression for the Franck-Condon factor vanishes [cf. Eq. (5.3)]. The quantum absorption tail, however, even with only one electronic transition taken into account, stretches to considerably higher energies.

VI. SUMMARY AND DISCUSSION

In this paper, we have studied the quantum lattice motion of short polyacetylene chains, described by the SSH model, in the ground and lowest excited electron states within the adiabatic approximation. Using both numerical calculations and analytical arguments, we have found that the number of lattice degrees of freedom whose dynamics is strongly modified by the interaction with electrons is small. In this respect the lattice dynamics of short chains is fundamentally different from that in the continuum limit. Moreover, we found that below a certain chain size (30 units for the standard polyacetylene parameters) the lattice dynamics is even further simplified, because the remaining relevant (nontrivial) lattice degrees of freedom become practically decoupled, although the dynamics of each of them is nonlinear. This has allowed us to perform a full quantum-mechanical calculation of the optical-absorption spectrum for photon energies for which only the lowest electronic transition is important. In particular, we have been able to study in detail the ''subgap'' smearing of the lowest rigid-band absorption peak as a result of the electron-phonon interaction (the ''subgap'' absorption spectrum).

This smearing may be defined as the energy difference between the peak position and the onset of absorption. Our calculations show a smearing of 0.5 eV, whereas the experiment shows 0.7 eV.[25] For a realistic comparison to the experiment, however, other important effects should be taken into account. First, the existence of higher excited electron configurations will further broaden the absorption spectrum. A proper inclusion of higher states, however, cannot be done within the adiabatic approximation and will be the subject of a forthcoming paper. Second, in reality, part of the smearing comes from higher dimensional effects, caused by interchain hopping. Most importantly, however, in practice appreciable additional broadening will arise from disorder in the electron conjugation length caused by conformational defects.[26] Recent studies[21] suggest that the distribution of conjugation lengths in polyacetylene is broad and has two peaks, one at $N\approx 40$ and one at $N\approx 80$. Within our modeling, such a distribution will lead to an important broadening, because a strong size dependence of the predicted absorption spectrum is observed. In particular, we have found that the absorption threshold ΔU varies by about 1.5 eV when N changes from 10 to 60 (see Fig. 9). Therefore, it seems that the combined effect of all broadening factors will, for the standard SSH parameters, lead to a predicted smearing of the absorption peak that is larger than the experimental value.

A solution to this problem may be the effect of the Cou-

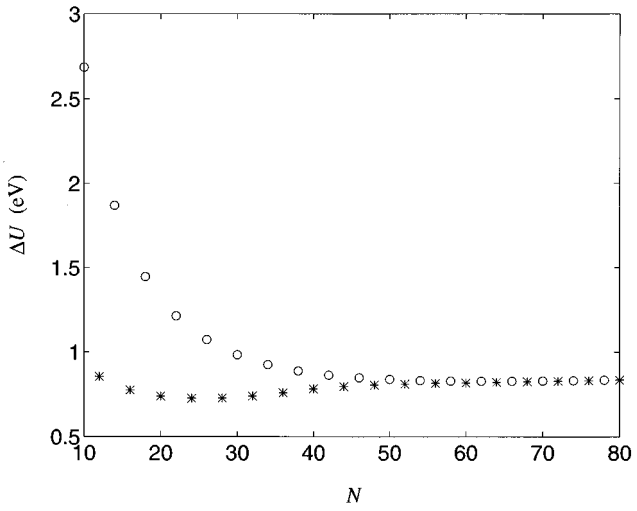

FIG. 9. The classical threshold for optical absorption, $\Delta U=\min(U_{\mathrm{ex}})-\min(U_{\mathrm{vac}})$, for polyacetylene rings with an even number of units N. The circles and asterisks distinguish between N indivisible and divisible by 4, respectively.

lomb interaction between the electrons. If we account for this coupling, the role of the electron-lattice interaction in the formation of the gap will diminish. In other words, the value of the electron-phonon coupling constant α necessary to fit the observed gap and lattice dimerization will be smaller when the Coulomb interaction is turned on. Accordingly, the effect of the quantum lattice fluctuations on the absorption spectrum and its size dependence will decrease.

In this paper, we have only considered polymer rings with $N=4k+2$ units (k integer) in detail. The case $N=4k$, which will naturally also occur in practice, differs from this mainly because no degeneracy occurs for the highest single-electron level in the chain with constant dimerization. Therefore, the effective potentials are somewhat different. In particular, the potential for the electronic ground state now has a cusp, while the potential for the electronic excited state has a nontrivial minimum only for $N\geqslant 36$. Nevertheless, the dynamics of the lattice degrees of freedom has similar simplicity as we found for $N=4k+2$, and the optical-absorption spectrum arising from it can be found in close analogy. As explained in Sec. II, we did not consider odd-N chains. Those have a solitonlike deformation with a midgap single-electron level in their ground state,[27] and their lattice dynamics accompanying optical absorption has to be studied separately.

As this is, to our knowledge, the first calculation of the quantum lattice dynamics and the optical absorption for short polymer chains, it is difficult to compare our results to previous theories dealing with subgap absorption. Earlier results were obtained in the continuum limit and, as discussed in the Introduction, are to a large extent approximate. Instead, we have made a comparison with a semiclassical calculation performed along the lines of Ref. 13, but adopted to the short chain case. This comparison clearly shows the limitations of the semiclassical approach [Fig. 7(b)].

In future work, we hope to include moderate electron-electron interactions and to apply our approach to the nonlinear optical response of conjugated polymers. The latter is of much interest, as the third-harmonic generation of degenerate-ground-state conjugated polymers has been claimed to be greatly enhanced by soliton-antisoliton pair production.[15–18]

ACKNOWLEDGMENTS

It is a pleasure to thank Professor G. Hadziioannou and Dr. P.F. van Hutten for stimulating discussions. This work is part of the research programs of the Stichting Scheikundig Onderzoek in Nederland (SON) and the Stichting voor Fundamenteel Onderzoek der Materie (FOM), which are financially supported by the Nederlandse Organisatie voor Wetenschappelijk Onderzoek (NWO).

APPENDIX: SEMICLASSICAL WAVE FUNCTIONS

In this appendix, we derive the semiclassical expressions for the wave functions describing large classically forbidden lattice fluctuations. This derivation is possible because of the (approximate) decoupling of the lattice degrees of freedom and is easier than the semiclassical calculation of the Green functions using the path-integral method.[13]

In the classically forbidden region of a one-dimensional potential $U(q)$, the wave function can be written

$$\phi(q)=\sqrt{w(q)}\exp\left(-\frac{S(q)}{\hbar}\right), \tag{A1}$$

where, by means of the standard WKB procedure, one identifies $S(q)$ with the Euclidean action,

$$S(q)=\left|\int_{q_0}^{q} p\,dq\right|, \tag{A2}$$

with $p(q)=\sqrt{2M(U(q)-E)}$ and q_0 the nearest turning point. To leading order in powers of $\hbar$, the preexponential factor is given by $w(q)=A(E)M/p(q)$, where the coefficient $A(E)$ is found by matching the semiclassical expression with the wave function in the classically accessible region. If the latter can also be described semiclassically, as is the case for the excited lattice states, then[28]

$$A(E)=\frac{1}{T(E)}, \tag{A3}$$

where $T(E)$ is the period of motion with energy E in the classically accessible region.

To find $A(E)$ for the lattice ground state, we match the semiclassical solution with the Gaussian function that describes the zero-point fluctuations near the minimum of U_{vac}. Now, somewhat different expressions are found for $S(q)$ and $w(q)$, because of the smallness of the ground-state energy. To see this, we insert Eq. (A1) into the Schrödinger equation for $\phi_{\|}(z)$,

$$\left(-\frac{\hbar^2}{2M}\frac{d^2}{dz^2}+V_{\mathrm{vac}}(z)\right)\phi_{\|}(z)=\varepsilon_{\|}\phi_{\|}(z), \tag{A4}$$

and expand in powers of $\hbar$, taking into account that the energy of the zero-point fluctuations $\varepsilon_{\|}=O(\hbar)$. Then, to zeroth order in $\hbar$ we obtain the Hamilton-Jacobi equation,

$$\frac{p_\parallel(z)^2}{2M} - V_{\rm vac}(z) = 0, \tag{A5}$$

where $p_\parallel(z) = dS_\parallel/dz$, while the first-order terms in $\hbar$ yield the equation for the probability current,

$$\hbar \frac{d}{dz}\left(w \frac{p_\parallel}{M}\right) = 2\varepsilon_\parallel w. \tag{A6}$$

The action $S_\parallel$ for the motion in $V_{\rm vac}(z)$ has to be calculated by numerical integration of $p_\parallel(z)$ [cf. Eq. (A2)]. The difference with the usual WKB procedure is that the energy of the lattice zero-point motion, $\varepsilon_\parallel$, is included in the last equation rather than the Hamilton-Jacobi equation (A5). Since we count energy from the minimum of $V_{\rm vac}(z)$, the classical momentum $p_\parallel(z)$ vanishes only at the minimum of the potential $z=a$, so that the solution is formally applicable for all z. In fact, the ability of the semiclassical solution to describe small fluctuations, as well as large ones, relies on the existence of a small parameter. To see this, we note that for the harmonic potential $V_{\rm vac} = (1/2)M\omega_\parallel^2(z-a)^2$, our procedure gives the exact ground-state wave function with $\varepsilon_\parallel = (1/2)\hbar\omega_\parallel$ [in this case $S_\parallel = (1/2)M\omega_\parallel(z-a)^2$ and $w(z) = \text{const}$]. Thus, small fluctuations are accurately described by the semiclassical solution if the anharmonicity of the potential is small over distances of the order of the zero-point fluctuation $\sqrt{\hbar/M\omega_\parallel}$ away from the minimum. For small anharmonicity, $\varepsilon_\parallel \approx (1/2)\hbar\omega_\parallel$, with $\omega_\parallel$ the frequency of small oscillations near the minimum of $V_{\rm vac}(z)$ at $z=a$. Then Eq. (A6) gives for the preexponential factor

$$w(z) = \frac{A}{p_\parallel(z)} \exp\left(M\omega_\parallel \int \frac{dz}{p_\parallel(z)}\right), \tag{A7}$$

and it is easy to check that $w(z)$ is regular at $z=a$. Since, for all practical purposes one can neglect the tunneling between the degenerate minima $z=\pm a$, the numerical coefficient A is found from the normalization condition

$$\int_0^\infty dz\, \phi_\parallel^2(z) = 1. \tag{A8}$$

To find the final lattice wave function $\phi'_\parallel(z)$ with energy $\varepsilon'_\parallel$ in the classically forbidden region of the harmonic potential $V = (1/2)M\omega_\parallel'^2 z^2$, the standard WKB approximation can be used and leads analytically to

$$\phi'_\parallel(z) = \left[\frac{M\omega'_\parallel}{2\pi p'_\parallel(z)}\right]^{1/2} \exp\left(-\frac{S'_\parallel(z)}{\hbar}\right), \tag{A9}$$

with

$$S'_\parallel(z) = \int_c^z dz\; p'_\parallel(z), \tag{A10a}$$

and

$$p'_\parallel(z) = M\omega'_\parallel \sqrt{z^2 - c^2}, \tag{A10b}$$

and c the right classical turning point determined by $\varepsilon'_\parallel = (1/2)M\omega_\parallel'^2 c^2$.

The initial wave function of the motion in the ''transverse'' directions, $\phi_\perp(\rho,\varphi)$, is the ground state of the two-dimensional harmonic oscillator with frequency $\omega_\perp$, which can be written in the ''semiclassical'' form

$$\phi_\perp(\rho,\varphi) = \left[\frac{M\omega_\perp}{\pi\hbar}\right]^{(1/2)} e^{-S_\perp/\hbar} \tag{A11a}$$

with the classical action

$$S_\perp = \frac{M\omega_\perp \rho^2}{2}. \tag{A11b}$$

Finally, for the ''transverse'' motion in the final lattice state, with the potential given by Eq. (3.9), we again use the WKB approximation. As both the semiclassical and the adiabatic approximation anyhow fail at small ρ, we neglect the centrifugal barrier for the $m=\pm 1$ states and obtain

$$R(\rho) = \left[\frac{M\omega'_\perp}{2\pi p'_\perp(\rho)}\right]^{1/2} \exp\left(-\frac{S'_\perp(\rho)}{\hbar}\right), \tag{A12}$$

with

$$S'_\perp(\rho) = \int_d^\rho d\rho\; p'_\perp(\rho), \tag{A13a}$$

and

$$p'_\perp(\rho) = -M\omega'_\perp \sqrt{(b-\rho)^2 - (b-d)^2}. \tag{A13b}$$

Here, d is the left classical turning point determined by $\varepsilon'_\perp = (1/2)M\omega_\perp'^2(b-d)^2$.

*Permanent address: Budker Institute of Nuclear Physics, Novosibirsk, 630090, Russia.

[1] *Conjugated Conducting Polymers*, edited by H. Kiess (Springer, Berlin, 1992).

[2] C. K. Chiang, C. R. Fincher, Y. W. Park, A. J. Heeger, H. Shirakawa, E. J. Louis, S. C. Gau, and A. G. MacDiarmid, Phys. Rev. Lett. **39**, 1098 (1977).

[3] I. D. W. Samuel, I. Ledoux, C. Dhenaut, J. Zyss, H. H. Fox, R. R. Schrock, and R. J. Silbey, Science **265**, 1070 (1994) and references therein.

[4] P. L. Burn, A. B. Holmes, A. Kraft, D. D. C. Bradley, A. R. Brown, R. H. Friend, and R. W. Gymer, Nature (London) **356**, 47 (1992).

[5] W. P. Su, J. R. Schrieffer, and A. J. Heeger, Phys. Rev. Lett. **42**, 1698 (1979); Phys. Rev. B **22**, 2099 (1980); **28**, 1138 (1983).

[6] A. J. Heeger, S. Kivelson, J. R. Schrieffer, and W. P. Su, Rev. Mod. Phys. **60**, 781 (1988).

[7] B. R. Weinberger, J. Kaufer, A. J. Heeger, A. Pron, and A. G. MacDiarmid, Phys. Rev. B **20**, 223 (1979).

[8] J. P. Sethna and S. Kivelson, Phys. Rev. B **26**, 3513 (1982).

[9] W. P. Su, Solid State Commun. **42**, 497 (1982).

[10] E. Fradkin and J. E. Hirsch, Phys. Rev. B **27**, 1680 (1983).

[11] A. Auerbach and S. Kivelson, Phys. Rev. B **33**, 8171 (1986).

[12] J. Yu, H. Matsuoka, and W. P. Su, Phys. Rev. B **37**, 10 367 (1988).

[13] A. Auerbach and S. Kivelson, Nucl. Phys. **B257**, 799 (1985).

[14] Z. Su and L. Yu, Phys. Rev. B **27**, 5199 (1983).
[15] M. Sinclair, D. Moses, D. McBranch, and A. J. Heeger, Phys. Scr. T **27**, 144 (1989).
[16] T. W. Hagler and A. J. Heeger, Chem. Phys. Lett. **189**, 333 (1992).
[17] C. Halvorson, T. W. Hagler, D. Moses, Y. Cao, and A. J. Heeger, Chem. Phys. Lett. **200**, 364 (1992).
[18] J. McElvain, N. Zhang, C. Halvorson, F. Wudl, and A. J. Heeger, Chem. Phys. Lett. **232**, 149 (1995).
[19] M. V. Berry, in *Geometric Phases in Physics*, edited by A. Shapere and F. Wilczek (World Scientific, Singapore, 1989), pp. 7–28.
[20] Y. Aharonov and A. Stern, Phys. Rev. Lett. **69**, 3593 (1992).
[21] R. Silbey, in *Conjugated Polymers and Related Materials*, edited by W. R. Salaneck *et al.* (Oxford, Oxford, 1993).
[22] H. Takayama, Y. R. Lin-Liu, and K. Maki, Phys. Rev. B **21**, 2388 (1980).
[23] S. Kivelson and W. K. Wu, Phys. Rev. B **34**, 5423 (1986).
[24] M. J. Rice and E. J. Mele, Chem. Scr. **17**, 121 (1981).
[25] N. Suzuki, M. Ozaki, S. Etemad, A. J. Heeger, and A. G. McDiarmid, Phys. Rev. Lett. **45**, 1209 (1980).
[26] See, e.g., J. Kürti and H. Kuzmany, Phys. Rev. B **44**, 597 (1991).
[27] W. P. Su, Solid State Commun. **35**, 899 (1980).
[28] L. D. Landau and E. M. Lifshitz, *Quantum Mechanics* (Pergamon, Oxford, 1977).